# Formation of the α-Aminoacrylate Intermediate Limits the Overall Reaction Catalyzed by *O*-Acetylserine Sulfhydrylase†

Eilika U. Woehl,‡ Chia-Hui Tai,§ Michael F. Dunn,‡ and Paul F. Cook*,§

*Department of Biochemistry, University of California, Riverside, California 92521-0129, and Department of Biochemistry and Molecular Biology, University of North Texas Health Science Center at Fort Worth, 3500 Camp Bowie Boulevard, Fort Worth, Texas 76107-2699*

*Received December 13, 1995; Revised Manuscript Received February 12, 1996*⊗

ABSTRACT: *O*-Acetylserine sulfhydrylase-A (OASS-A) catalyzes the final step in the synthesis of L-cysteine, *viz*., the β-substitution of acetate in *O*-acetyl-L-serine (OAS) by sulfide via a ping-pong kinetic mechanism. Rapid-scanning stopped-flow and single-wavelength absorbance and fluorescence stopped-flow experiments were carried out to obtain information on the location and amount of limitation of rate-determining steps for the overall reaction and the individual half-reactions of OASS-A. The first half-reaction, conversion of OAS to the α-aminoacrylate intermediate and acetate, is rate-limiting for the overall reaction catalyzed by OASS-A. No intermediates are detected within the second half-reaction, and thus rate constants for all steps must be ≥1000 $s^{-1}$ at the lowest sulfide concentration used. Within the first half reaction, formation of the external Schiff base ($K_{association}$ = 0.2 $mM^{-1}$) is observed in the first few milliseconds, followed by its slower conversion to the α-aminoacrylate intermediate with a rate constant of 300 $s^{-1}$, close to the value of 130 $s^{-1}$ obtained for $V/E_t$ [Tai, C.-H., Nalabolu, S. R., Jacobson, T. M., Minter, D. E., & Cook, P. F. (1993) *Biochemistry 32*, 6433−6442]. Addition of L-cysteine to OASS-A results in a rapid formation of the external Schiff base ($K_{association}$ = 6.7 $mM^{-1}$), followed by transient formation of the α-aminoacrylate intermediate with a slightly lower rate (70−100 $s^{-1}$) compared to OAS. The α-aminoacrylate intermediate decays to generate a species absorbing maximally at 418 nm, resulting from attack of the cysteine thiol to give a thiol ether in external Schiff base linkage with the active site PLP.

The synthesis of L-cysteine in *Salmonella typhimurium* proceeds via a two-step enzymatic pathway (Kredich & Tomkins, 1966). In the first step, catalyzed by serine transacetylase, the β-hydroxyl group of L-serine is activated for elimination by acetylation using acetyl-CoA as the acetyl donor. The *O*-acetyl-L-serine intermediate then undergoes a β-substitution reaction catalyzed by the PLP-dependent[1] *O*-acetylserine sulfhydrylase in which acetate is eliminated and replaced by sulfide to give L-cysteine.

The kinetic mechanism for OASS-A, an isozyme thought to operate under aerobic growth conditions, has recently been determined using initial velocity studies with several alternative substrates (Tai et al., 1993), extending earlier work carried out by Cook and Wedding (1976). The enzyme has a classical ping-pong kinetic mechanism with competitive inhibition by both substrates indicative of E:sulfide and F:OAS dead end complexes.

The *O*-acetylserine sulfhydrylase (OASS) reaction has been studied using a number of spectral probes including UV−visible, fluorescence, circular dichroism, and $^{31}P$ NMR spectroscopy. The ultraviolet−visible spectrum of OASS-A exhibits an absorption maximum at 412 nm due to the formation of a protonated Schiff base between an active site lysine and the active site PLP (Cook & Wedding, 1976; Cook et al., 1992). Addition of OAS to the native enzyme results in the disappearance of the absorbance at 412 nm and the appearance of new absorption maxima at 330 and 470 nm indicative of the formation of a protonated Schiff base between PLP and α-aminoacrylate upon the β-elimination of acetate from OAS (Cook & Wedding, 1976; Schnackerz et al., 1979; Cook et al., 1992). The addition of L-cysteine, L-alanine, or glycine to OASS results in the shift in $\lambda_{max}$ of 412 nm for the internal Schiff base to 418 nm resulting from the formation of the external Schiff base (Schnackerz et al., 1995). The addition of L-serine or *O*-methyl-D,L-serine gives a decrease in the absorbance of unliganded enzyme at 412 nm by about 50% and 20%, respectively, concomitant with an increase in the absorbance at 320 nm, and a shift in the $\lambda_{max}$ of the remaining visible absorbance to 418 nm. The data obtained with serine or *O*-methylserine are suggestive of establishing an equilibrium between different tautomeric forms of an external Schiff base (Schnackerz et al., 1995). The pH dependence of dissociation constants for decomposition of the external Schiff bases obtained from the above spectral changes suggests that the α-amine of the amino acid and an enzyme group that hydrogen-bonds the side chain functional group must be unprotonated for optimal formation

† This work was supported by grants to P.F.C. and M.F.D. from the National Science Foundation (MCB 9405020 and MCB 9218901) and to P.F.C. from the Robert A. Welch Foundation (BK-1031), and by Grant CRG. 900519 from the North Atlantic Treaty Organisation Scientific Affairs Division to P.F.C. and Klaus D. Schnackerz of the University of Würzburg.

‡ University of California, Riverside.

§ University of North Texas Health Science Center at Fort Worth.

⊗ Abstract published in *Advance ACS Abstracts,* April 1, 1996.

[1] Abbreviations: Mes, 2-(*N*-morpholino)ethanesulfonic acid; Ches, 2-(*N*-cyclohexylamino)ethanesulfonic acid; SB, Schiff base; DTNB, 5,5′-dithiobis(2-nitrobenzoate); RSSF, rapid-scanning stopped-flow; OAS, *O*-acetyl-L-serine; OASS, *O*-acetylserine sulfhydrylase; PLP, pyridoxal 5′-phosphate.

0006-2960/96/0435-4776$12.00/0 © 1996 American Chemical Society

of the external Schiff base. In addition, when L-cysteine is the amino acid, the side chain thiol must be protonated for optimal external Schiff base formation. There is no change in the far-UV CD upon addition of OAS, but a significant change upon addition of either cysteine or serine, thought to suggest a closing of the active site (Schnackerz et al., 1995). The $^{31}$P NMR chemical shift is increased from 5.2 to 5.3 ppm, signaling a tighter interaction at the 5′-phosphate upon formation of the cysteine external Schiff base, while no change is observed upon addition of OAS. In the case of serine, the $^{31}$P NMR signal is decreased to 4.4 ppm, suggesting a loosening of the binding at the 5′-phosphate. The fluorescence spectrum in the presence of serine exhibits an enhancement of the long-wavelength energy transfer band (McClure & Cook, 1994) consistent with the amount of external Schiff base present (Schnackerz et al., 1995).

The pH dependence of the ultraviolet−visible spectrum in the absence and presence of OAS indicates that the p$K_a$ values for the Schiff base nitrogen in free enzyme and the α-aminoacrylate intermediate are greater than 10 (Cook et al., 1992). In addition, these authors showed via $^{31}$P NMR that the phosphate is dianionic over the pH range 6−10. Finally, an OAS deacetylase activity was identified in which the active site lysine that was in Schiff base with PLP displaces α-aminoacrylate to regenerate free E and produce pyruvate and ammonia. The pH dependence of the deacetylase activity gave a p$K_a$ for the active site lysine of 8.2.

The pH dependence of kinetic parameters using natural and alternative reactants has also been measured to obtain information on the chemical mechanism of OASS-A (Tai et al., 1995) A general mechanism (Scheme 1) is proposed for OASS in which OAS binds with its α-amine unprotonated to carry out a nucleophilic attack on C4′ of the protonated Schiff base, and with the acetyl carbonyl hydrogen-bonded to a protonated enzyme group, which aids in the β-elimination of acetate. The enzyme lysine, that was in Schiff base linkage with the active site PLP, deprotonates the α-carbon in the β-elimination reaction, and a proton is likely released with the acetate product. Sulfide likely binds as $HS^-$ to undergo nucleophilic attack on the α-aminoacrylate intermediate, followed by protonation of the α-carbon by the enzyme lysine. The $HS^-$ may be hydrogen-bonded to the enzyme group that assists in the β-elimination of acetate.

Virtually nothing is known of the location and amount of limitation of rate-determining steps along the reaction pathway. In the present study, rapid scanning stopped-flow spectrophotometric studies are carried out to provide information on the location of slow steps in both half reactions. Overall, the first half reaction limits, with formation of the external Schiff base, one of the slow steps. No intermediates could be detected in the second half reaction.

## MATERIALS AND METHODS

*Chemicals*. *O*-Acetyl-L-serine and $Na_2S$ were obtained from Sigma. All other reagents and chemicals were obtained from commercially available sources and were of the highest quality available.

*Enzyme*. *O*-Acetylserine sulfhydrylase-A from *Salmonella typhimurium* LT-2 was purified by the method of Hara et al. (1990) as modified by Tai et al. (1993). The enzyme preparation used in this study was >95% pure on the basis of SDS−PAGE. The enzyme had a specific activity of 800 units/mg with sulfide as the second substrate, and assayed using a sulfide ion selective electrode (Hara et al., 1990). The protein concentration of the purified enzyme was determined from the absorbance of the Schiff base between the active site lysine and PLP at 412 nm, using an extinction coefficient of 7600 $M^{-1}$ $cm^{-1}$ (Cook et al., 1992).

*Ultraviolet−Visible Spectra*. All spectra were collected at 25 °C in reaction cuvettes 1 cm in path length and 1 mL in volume. Absorption spectra were measured utilizing a Hewlett Packard 8452A diode array spectrophotometer. Measurements were made using 100 mM Mes, pH 6.5. All assay buffers used in these studies were titrated with KOH.

*Rapid-Scanning and Single-Wavelength Stopped-Flow*. The RSSF system used in these studies is composed of a Durrum D-110 rapid-mixing stopped-flow device and a Princeton Applied Research multichannel analyzer with a 1214 photodiode array detector (Dunn et al., 1979; Koerber et al., 1983). In each RSSF experiment, a set of 25 scans is collected. For all data sets, 500 pixels were scanned with a repetitive scanning time of 8.544 ms. The scans are converted into OD units utilizing a 100% transmittance spectrum (buffer solution alone) and the diode array dark current spectrum. Both spectra were recorded prior to each of the experiments using the appropriate buffer solution as a blank. The 25 scans in each experiment are collected at specific intervals defined by the selected timing sequence. One of three different timing sequences was used for an individual data set. The timing sequences are defined below.

Timing sequence 1 made use of a total acquisition time of 0.34 s. The 25 scans adhere to the following time points after flow is stopped: 2, 0.017 s; 4, 0.034 s; 6, 0.051 s; 8, 0.068 s; 10, 0.085 s; 12, 0.12 s; 15, 0.17 s; 20, 0.26 s; and 25, 0.34 s.

Timing sequence 3 made use of a total acquisition time of 1.71 s. The 25 scans adhere to the following time points after flow is stopped: 2, 0.017 s; 4, 0.034 s; 6, 0.06 s; 8, 0.084 s; 10, 0.13 s; 11, 0.18 s; 12, 0.23 s; 15, 0.38 s; 20, 0.85 s; and 25, 1.71 s.

Timing sequence 11 made use of a total acquisition time of 119.6 s. The 25 scans adhere to the following time points after flow is stopped: 4, 0.034 s; 6, 0.46 s; 10, 2.14 s; 15, 12.8 s; 20, 55.5 s; and 25, 119.6 s.

Single-wavelength absorbance and fluorescence stopped-flow studies were performed using a Durrum D-110 stopped-flow device with a sample handling unit from Applied Photophysics and a photomultiplier detection system. Single-wavelength time courses were fitted using the Marquardt−Levenberg algorithm to an equation of the following general form:

$$A_t = A_\infty \pm \sum A_i \exp(-t/\tau_i) \quad (1)$$

$A_t$ and $A_\infty$ are the absorbance values at time $t$ and time ∞, respectively. $A_i$ and $\tau_i$ represent the $i$th amplitude and relaxation time, respectively. All time courses were collected under pseudo-first-order conditions.

*Peak-Fitting Analysis of RSSF Spectra*. Single spectra for specific time points of the RSSF spectral set were extracted into separate files and analyzed with the help of a commercial peak-fitting software (PeakFit, Version 3.1/Jandel Scientific). The software applies the Marquardt−Levenberg algorithm to fit a spectrum to a sum of peaks.

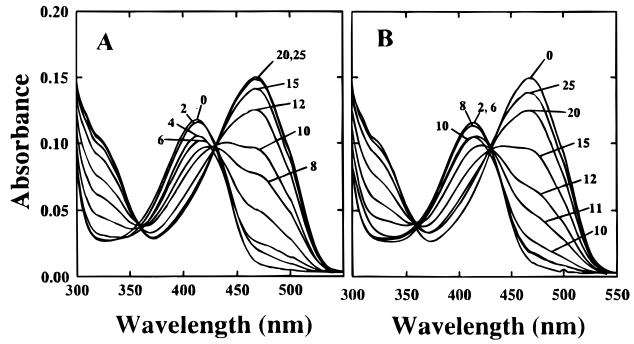


FIGURE 1: Rapid-scanning stopped-flow spectra obtained upon reaction of OASS with OAS (A), and upon reaction of OASS-A premixed with OAS with $HS^-$ (B). In both panels, spectrum 0 is with enzyme alone. The other numbers refer to timing sequence 3 for panel A and timing sequence 1 for panel B. Concentrations: (A) [OASS-A] = 10 $\mu$M sites and [OAS] = 1 mM; (B) [OASS-A] = 10 $\mu$M sites, [OAS] = 1 mM, and [$HS^-$] = 0.25 mM. All three reactions were run in 100 mM Mes, pH 6.5, with [$K^+$] = 100 mM.

The shape of each of the individual peak areas was described using a lognormal equation with four independent parameters [as described by Siano and Metzler (1969), Siano (1972), and Metzler et al. (1985, 1991); see also Houben et al. (1989), Houben and Dunn (1990), and Woehl and Dunn (1995)]. To correct for light scattering and base line shifts, a curve of the general form $y = ax^{-4} + c$ was used. The parameters for the latter curve were estimated from absorbance measurements in the 600−800 nm region, where PLP-bound intermediates do not contribute to the absorbance. The small scatter curve has been eliminated for clarity.

## RESULTS

*Rapid-Scanning Stopped-Flow*. RSSF measurements were carried out to obtain information on the identity and rates of appearance and decomposition of transients in the pre-steady-state time course of the OASS reaction. During the reaction of OASS with OAS, the reactant in the first half reaction of the ping-pong mechanism gives the spectra shown in Figure 1A. Spectrum 0 is the spectrum for OASS prior to adding OAS. Upon addition of OAS, the 412 nm absorption band of free enzyme resulting from the internal Schiff base (Cook et al., 1992) is shifted slightly to higher wavelength as seen in the value of the $\lambda_{max}$ for spectrum 2 vs spectrum 0, and the lack of a single isosbestic point for spectra 0−6. The rapid shift in the wavelength which signals formation of the external Schiff base of OAS (Schnackerz et al., 1995) is followed by a decrease in the absorbance at 412−420 with the concomitant appearance of new bands at 330 and 470 nm resulting from formation of the α-aminoacrylate intermediate (Cook et al., 1992). Spectrum 25 shows the equilibrium mixture of species after reaction for about 1 s. Peak-fitting analysis using lognormal distribution curves of some of the individual spectra of the RSSF spectral set was performed. The fit for spectrum 2 is shown in Figure 2A. The analysis identifies three peaks with $\lambda_{max}$ values of 413.5 nm (internal plus external Schiff bases) and 330 and 470 nm (both reflecting the presence of the α-aminoacrylate intermediate). The fit for spectrum 8 again gives a mixture of two species, external Schiff base and α-aminoacrylate intermediate, but with the latter predominant (Figure 2B).

Extinction coefficients for the observed species were calculated from the decomposed spectra shown in Figure 2.

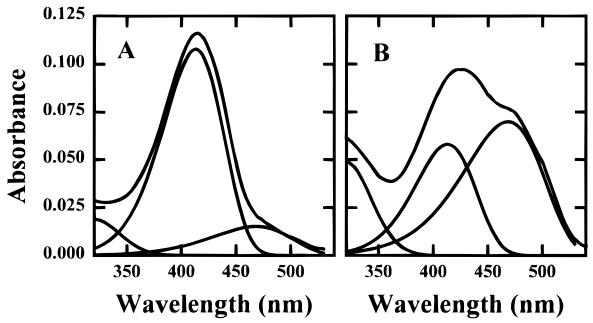


FIGURE 2: Theoretical lognormal fits for two spectra from Figure 1A. Panel A is for spectrum 2, and panel B is for spectrum 8.

The $\epsilon_{470}$ of the α-aminoacrylate intermediate is estimated at 10.5 $mM^{-1}$ $cm^{-1}$, similar to the value of 9.8 $mM^{-1}$ $cm^{-1}$ estimated from equilibrium UV−visible spectra (Cook et al., 1992). The 330 nm band also likely reflects the α-aminoacrylate intermediate, since it exhibits rate constants identical to those estimated from the 470 nm band, and the ratio of absorbancies at 470 and 330 nm is constant during the course of the reaction. It is suggested that the 330 nm band is due to an electronic transition of the α-aminoacrylate and likely represents a second tautomeric form of the intermediate, or a form in which the intramolecular hydrogen bond between the imine nitrogen and the 3-hydroxyl of PLP is for some reason not allowed. In the case of the closely related tryptophan synthase, only a 350 nm band of the α-aminoacrylate intermediate together with a shoulder extending beyond 500 nm is observed (Miles, 1979). An $\epsilon_{330}$ of 7 $mM^{-1}cm^{-1}$ is estimated for the α-aminoacrylate intermediate in tryptophan synthase.

When the α-aminoacrylate intermediate is preformed by mixing OASS and OAS, and then reacted with sulfide, the spectra shown in Figure 1B are obtained. Spectrum 0 depicts the spectrum of the α-aminoacrylate intermediate after reaction of OASS with OAS, while the first spectrum after mixing, spectrum 2 in Figure 1B, shows a mixture dominated by a species that absorbs at 412 nm (internal Schiff base) with a small amount of the α-aminoacrylate intermediate. After a delay in which sulfide is depleted, the spectral changes in 10−25 are determined by the re-formation of the α-aminoacrylate intermediate species from the internal Schiff base and excess OAS.

Addition of L-cysteine to OASS is known to result in the formation of an external Schiff base (Schnackerz et al., 1995). Rapid-scanning stopped-flow spectra obtained upon addition of L-cysteine to OASS are presented in Figure 3A. The spectra show a rapid formation of the external SB species reflected in a red shift in the $\lambda_{max}$, followed by the slow decay of external Schiff base to form the α-aminoacrylate intermediate with absorption maxima at 330 and 470 nm. Figure 3B depicts the same reaction at longer times showing the very slow decay of the α-aminoacrylate over the longer time period.

Addition of L-serine to OASS is known to result in the formation of an external Schiff base with spectral bands at 320 and 418 nm (Schnackerz et al., 1995). Rapid-scanning stopped-flow spectra obtained upon addition of L-serine to OASS are shown in Figure 4. Spectrum 0 depicts enzyme alone, while spectra 2−25 show a red shift in the $\lambda_{max}$ and the concomitant appearance of a second absorption band at 320 nm resulting from the external SB formed with L-serine.

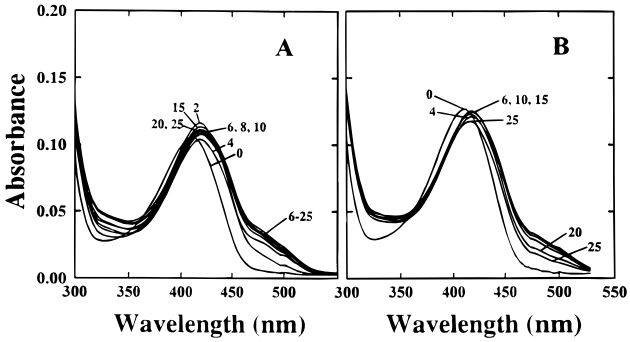


FIGURE 3: Rapid-scanning stopped-flow spectra obtained upon reaction of OASS with L-cysteine. In both panels, spectrum 0 is with enzyme alone. Panel A shows the reaction using timing sequence 1, and panel B shows the same reaction using timing sequence 11. Concentrations: (A) [OASS-A] = 8.5 $\mu$M sites and [L-cysteine] = 1 mM. (B) [OASS-A] = 10 $\mu$M sites and [L-cysteine] = 1 mM. All reactions were run in 100 mM Ches, pH 9.5, with [$K^+$] = 100 mM.

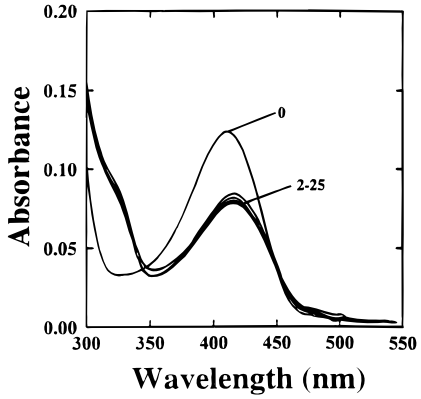


FIGURE 4: Rapid-scanning stopped-flow spectra obtained upon reaction of OASS with L-serine. Spectrum 0 is with enzyme alone. Timing sequence 1 was used. Concentrations: [OASS-A] = 10 $\mu$M sites and [L-serine] = 50 mM. Reactions were carried out in 100 mM Ches, pH 9.5, with [$K^+$] = 100 mM.

The reaction takes place within the dead time of the instrument.

*Single-Wavelength Stopped-Flow Studies*. In order to better measure the formation and decay of individual intermediates, single-wavelength stopped-flow experiments were carried out. The appearance of the α-aminoacrylate intermediate upon mixing OAS with OASS was monitored at 470 nm (or 330 nm, data not shown) as a function of the concentration of OAS, Figure 5A. Time courses were analyzed with curve-fitting software and the relaxation rate parameters determined. All curves were best fitted using a single exponential. A plot of the dependence of the relaxation rate ($1/\tau$) on the concentration of OAS is shown in Figure 5B. A mechanism of the type A + B ↔ C → D was used, where A is free enzyme, B is OAS, C is the external Schiff base, and D is the α-aminoacrylate intermediate. The concentration dependence of the relaxation rate on the concentration of OAS is given in eq 2 (Bernasconi, 1976) using rate constant designations given in the limiting mechanism in Scheme 3:

$$1/\tau_2 = k_5 K_{ext}[\mathrm{OAS}]/(1 + K_{ext}[\mathrm{OAS}]) \qquad (2)$$

where $K_{ext}$ is equal to $K_1K_3$, $K_1$ is $k_1/k_2$, and $K_3$ is $k_3/k_4$. Estimated values of $K_{ext}$ and $k_5$ based on the data in Figure 5B are 0.18 $mM^{-1}$ and 300 $s^{-1}$, respectively, while for the

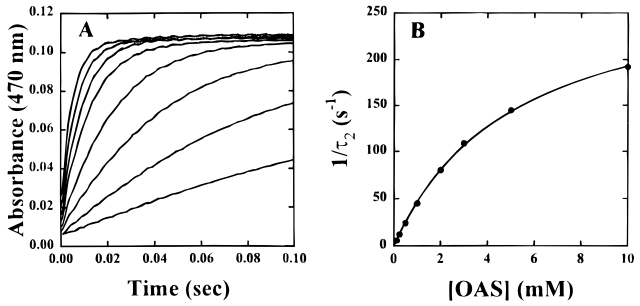


FIGURE 5: Single-wavelength absorbance time courses for the appearance of the α-aminoacrylate intermediate monitoring the absorbance at 470 nm upon reaction of OASS with OAS. All reactions were carried out in 100 mM Mes, pH 6.5, with [$K^+$] = 78 mM and [OASS] = 5 $\mu$M sites. Concentrations of OAS are as follows in order for time courses exhibiting the slowest to the fastest rates: (A) 0.05, 0.1, 0.25, 0.5, 1, and 2.5 mM OAS. (B) Dependence of the relaxation rates for the formation of the band at 470 nm on the concentration of OAS.

appearance of the 330 nm band, values are 0.22 $mM^{-1}$ and 270 $s^{-1}$, respectively.[2] Complete saturation of the rate is not reached over the range of OAS concentrations used.

Formation of the external Schiff base is accompanied by an increase in the fluorescence emission at 500 nm (excitation at 290 nm) resulting from delayed fluorescence of the ketoenamine tautomer of the external Schiff base. Stopped-flow of the 500 nm fluorescence signal upon mixing OAS with OASS can thus be used to obtain an additional estimate of the rate of appearance of α-aminoacrylate intermediate. Time courses for the decay of 500 nm fluorescence can be best fitted by an equation reflecting a single exponential (data not shown). The dependence of the relaxation rate on the concentration of OAS shows a tendency toward saturation over the range used (data not shown). Parameters determined from the fluorescence data are 0.16 $mM^{-1}$ and 310 $s^{-1}$ for $K_{ext}$ and $k_5$, respectively.

Reaction of the preformed α-aminoacrylate intermediate with the second substrate, $HS^-$, was monitored at 470 nm in a single-wavelength stopped-flow experiment. The decay of the 470 nm band is too rapid to be measured even at low concentrations of $HS^-$, and reaction is complete in the mixing time. The relaxation rate for the disappearance of the absorbance at 470 nm must be ≥1000 $s^{-1}$.

The formation and decay of the cysteine external Schiff base and the formation of the α-aminoacrylate intermediate were monitored by single wavelength stopped-flow experiments. Figure 6A shows the time courses for the formation of the α-aminoacrylate intermediate at 470 nm (also obtained at 330 nm, data not shown). The time courses are best fitted by a single-exponential equation. The dependence of $1/\tau$ on the concentration of L-cysteine is described by a hyperbola (Figure 6C), and data were fitted assuming a rapidly equilibrating first step followed by a slower second step according to eq 2. Estimates of the equilibrium constant ($K_{ext2}$)[3] for the first step and the rate constant $k_8$ for the second step are 6.7 $mM^{-1}$ and 110 $s^{-1}$, while values of 6.8 $mM^{-1}$ and 71 $s^{-1}$, respectively, are obtained for the 330 nm data (not shown). [A value of 8 $mM^{-1}$ has been estimated for $K_{ext2}$ from equilibrium titrations (Schnackerz et al., 1995), in excellent agreement with the present study.] The fluores-

[2] Standard errors on the rate constants are on the order of 20%.
[3] $K_{ext2} = K_{12}K_{10}$, where $K_{12} = k_{12}/k_{11}$, and $K_{10} = k_{10}/k_9$.

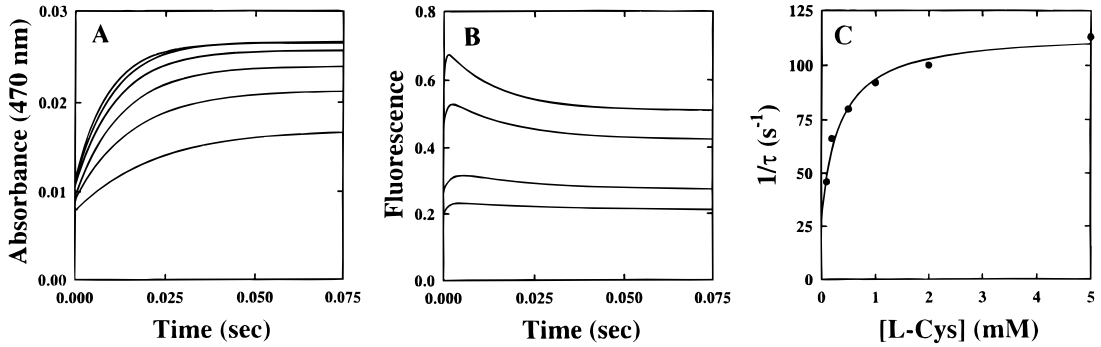


FIGURE 6: Single-wavelength absorbance time courses for the appearance of the α-aminoacrylate intermediate monitoring the absorbance at 470 nm upon reaction of OASS with L-cysteine. All reactions were carried out in 100 mM Ches, pH 9.5, with $[K^+] = 100$ mM and [OASS] = 10 $\mu$M sites. Concentrations of L-cysteine are as follows in order for time courses exhibiting the slowest to the fastest rates: (A) 0.1, 0.2, 0.5, 1, 2, and 5 mM L-cysteine. (B) Fluorescence time courses (excitation at 284 nm) at 0.1, 0.2, 0.5, and 1 mM L-cysteine. (C) Dependence of the relaxation rates for the formation of the band at 470 nm from (A) on the concentration of L-cysteine.

cence excitation spectrum with emission at 500 nm for a mixture of OASS and L-cysteine shows excitation peaks at 284 and 420 nm. The peak at 420 nm is 5.6-fold higher than for a solution of enzyme alone. The 500 nm fluorescence signal was used to follow the formation and decay of the external Schiff base, and selected time courses are shown in Figure 6B. The formation of the external Schiff base species is very fast (700−1000 $s^{-1}$). The disappearance of the external Schiff base is slower and gives a relaxation rate of 66 $s^{-1}$ at 1 mM L-cysteine, consistent with the above estimated parameters.

The time course for appearance of the 500 nm fluorescence emission band ($\lambda_{ex} = 298$ nm) for reaction of OASS with 5 mM L-serine is very rapid, giving an estimated rate constant of ~800 $s^{-1}$, a value at the limit of detection (data not shown).

*Diode Array UV−Visible Spectroscopy*. Addition of OAS to OASS results in formation of the α-aminoacrylate intermediate, a species which absorbs at 470 nm. Addition of L-cysteine to the α-aminoacrylate intermediate results in the disappearance of absorbance at 470 nm, (data not shown), suggesting that L-cysteine reacts with the intermediate to form a new product. At the end of the reaction, an external Schiff base, presumably with the new product, that absorbs at 418 nm is present (data not shown), and the thiol group of L-cysteine can no longer be titrated with DTNB. Addition of OAS results in the immediate reappearance of the α-aminoacrylate intermediate (data not shown). The OASS-A isozyme has also been reported to catalyze a deacetylase activity, where the α-aminoacrylate intermediate is converted to pyruvate and ammonia (Cook et al., 1992). Although the rate of the deacetylase activity is significant under the above conditions, it is still 3-fold slower than the rate of disappearance of the 470 nm intermediate in the presence of 1 mM L-cysteine.

## DISCUSSION

*Rapid-Scanning Stopped-Flow*. The first half reaction, conversion of OAS to the α-aminoacrylate intermediate and acetate, is rate-limiting for the overall reaction catalyzed by *O*-acetylserine sulfhydrylase. Addition of sulfide to the preformed α-aminoacrylate intermediate results in regeneration of the internal Schiff base within the instrument dead time (~8 ms) of the rapid-scanning stopped-flow, and a delay in appearance of any intermediates until the added sulfide has been depleted. No intermediates in the second half reaction, conversion of the α-aminoacrylate intermediate and sulfide to cysteine, are detected.

Within the first half reaction, however, formation of the external Schiff base is observed as a shift in the $\lambda_{max}$ of the internal Schiff base which occurs in the first few milliseconds of the RSSF experiment. Formation of the external Schiff base must occur via *gem*-diamine intermediates, one of which is pictured in Scheme 1. Lack of observation of any additional intermediates absorbing in the 320−350 nm range indicates a very rapid formation and decay of the *gem*-diamine intermediates in the OASS-A reaction. The rapid formation of the external Schiff base is followed by its slower conversion to the α-aminoacrylate intermediate. Thus, the slow step in the first half reaction is the α,$\beta$-elimination of acetate catalyzed by the active site lysine that was in Schiff base linkage with PLP (Scheme 1). In agreement with the RSSF data, a deuterium isotope effect on $V/K_{OAS}$ of about 2.5 is obtained at pH 6.5 using OAS-2-D (unpublished results of C.-C. Hwang in the PFC lab).

The results obtained with cysteine, the reactant in the reverse of the OASS-A reaction, are surprising. Although isotope exchange at equilibrium is obtained for the $HS^-$ cysteine exchange (Cook & Wedding, 1976), no initial rate of OAS appearance has been observed even at 100 times the concentration of OASS used in the direction of cysteine formation (Tai et al., 1993). Also, cysteine addition to OASS-A results in the formation of an external Schiff base, not the α-aminoacrylate intermediate (Schnackerz et al., 1995). In the pre-steady-state, however, cysteine addition to OASS-A clearly results in the formation of the α-aminoacrylate intermediate absorbing at 330 and 470 nm, albeit slowly and to a lesser extent than observed with OAS. The formation of the α-aminoacrylate intermediate, however, is followed by the slow, on the pre-steady-state time scale, disappearance of the the α-aminoacrylate intermediate. Coupled to the results obtained from steady-state experiments that show cysteine can replace sulfide as a reactant, the data suggest that the transient α-aminoacrylate intermediate formed is converted to a new product that is likely a thiol ether according to Scheme 2. In agreement with the suggested mechanism, addition of cysteine to the α-aminoacrylate intermediate results in a loss of the ability to detect the cysteine thiol with DTNB.

Schnackerz et al. (1995) have reported the dissociation constant for decomposition of the cysteine external Schiff base obtained from spectral changes observed upon addition

Scheme 1

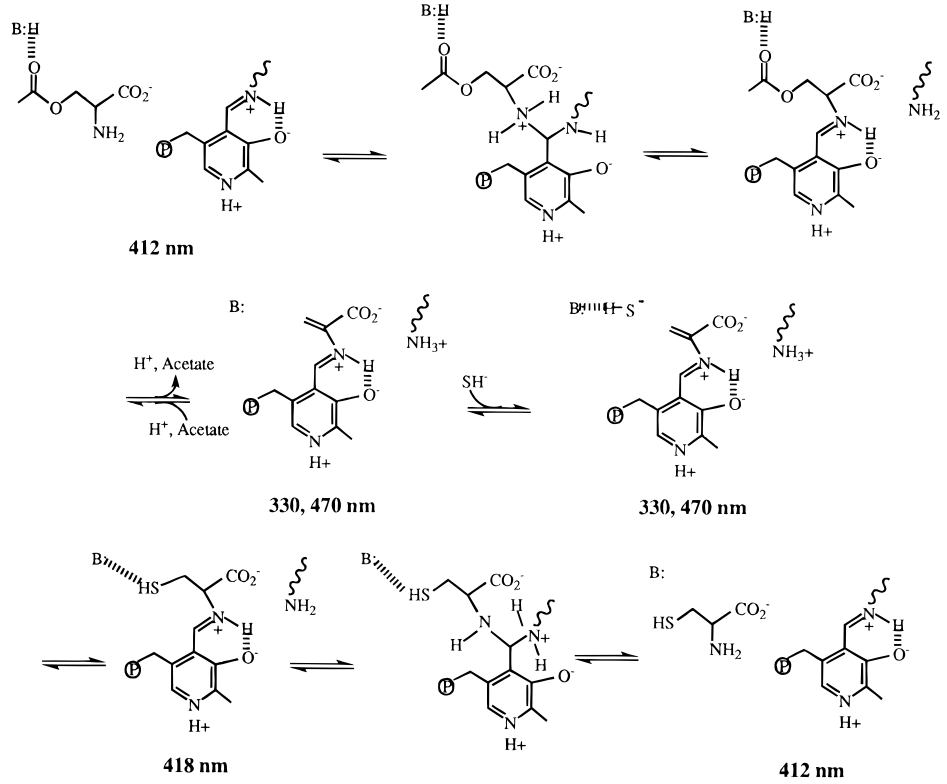


Scheme 2

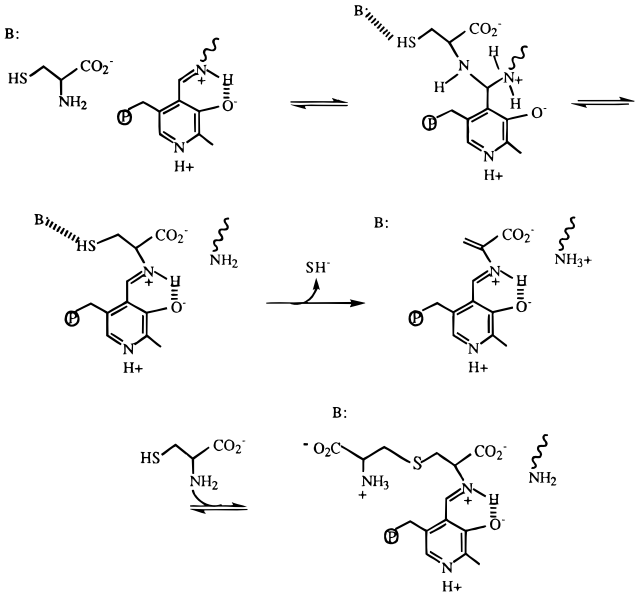

Scheme 3

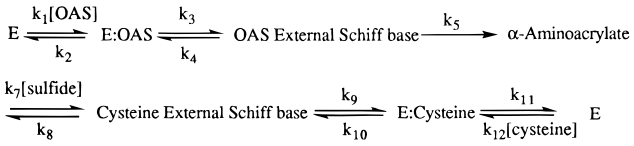


of L-cysteine to OASS-A. The above interpretation, however, indicates that the external Schiff base formed is likely with the thiol ether product and not L-cysteine. The pH dependence of the dissociation constant has been interpreted to suggest that the α-amino group of L-cysteine and an enzyme group that hydrogen-bonds to the side chain functional group must be unprotonated, while the side chain thiol must be protonated for optimal external Schiff base formation (Scheme 3). This interpretation is still valid despite the change in mechanism resulting in formation of the thiol ether external Schiff base. Once the cysteine external Schiff base is formed, it is committed to eliminate $HS^-$ and to add the second molecule to form the thiol ether external Schiff base. As a result, the observed pH dependence of the measured dissociation constant is that for formation of the cysteine external Schiff base.

Experiments carried out with L-serine demonstrated that no intermediates other than the serine external Schiff base absorbing at 320 and 418 nm (Schnackerz et al., 1995) were detected. However, these data are consistent with observations made with OAS and cysteine, and show that formation and decay of the *gem*-diamine intermediates are too rapid to detect, occurring in the mixing time of the stopped-flow.

*Single-Wavelength Stopped-Flow*. The quantitative data obtained from the present studies are limited as a result of the rapidity of the rate processes studied. A *gem*-diamine intermediate is expected to precede the external Schiff base with reactant, (Scheme 1). No *gem*-diamine intermediate is visualized under any experimental conditions, and thus formation and decay of the *gem*-diamine intermediates must be very rapid, and the equilibrium between these intermediates and the external Schiff base must be far toward the latter. The external Schiff base is also rapidly formed, and accumulates in the pre-steady-state. An estimate of 0.2 $mM^{-1}$ for the association constant for formation of the OAS external Schiff base is obtained from the dependence of the observed rate constant on the concentration of OAS. In addition, the rate of conversion of the OAS external Schiff base to the α-aminoacrylate intermediate has been well-determined, 300 $s^{-1}$, and the latter is only slightly higher than the value of 130 $s^{-1}$ obtained for $V/E_t$ for the overall reaction at pH 7 (Tai et al., 1993). No intermediates are

observed in the second half reaction in the direction of cysteine synthesis, suggesting that all steps in the second half reaction occur (at the lowest sulfide concentration used) with a rate constant $\geq 1000$ $s^{-1}$. In agreement with the finding of a rapid second half reaction, a value of $>107$ $M^{-1}$ $s^{-1}$ is obtained for $V/K_{sulfide}E_t$, near the diffusion limit (Tai et al., 1993).

Although no intermediates are detected in the second half reaction in the direction of cysteine formation, beginning with cysteine, a rapid formation of the external Schiff base is observed with an association constant of 6.7 $mM^{-1}$. An estimate of the rate constant for formation of the external Schiff base, obtained by monitoring 500 nm fluorescence, is $700-1000$ $s^{-1}$. Decay of the cysteine external Schiff base occurs with a rate constant of about $70-100$ $s^{-1}$ monitoring absorbance or fluorescence. In agreement with the estimated rate constant of $700-1000$ $s^{-1}$ for formation of the cysteine external Schiff base, an estimated rate constant of $\sim 800$ $s^{-1}$, is obtained for the formation of the serine external Schiff base.

*Comparison with Tryptophan Synthase*. Sequence comparisons indicate that OASS-A and the $\beta$-subunit of tryptophan synthase (here designated as $\beta_2$) both belong to the $\beta$-family of PLP enzymes (Alexander et al., 1994). There is 19% sequence identity between the two proteins, and the sequence similarity is 40%, indicating that the overall folding of OASS-A and $\beta_2$ give similar structures. The similarities in the chemistry of the reactions catalyzed by OASS-A and $\beta_2$ suggest, *a priori*, that the catalytic mechanism of OASS-A and $\beta_2$ should have many features in common. Consequently, it is surprising to find that the chemistry of catalysis diverges significantly at two points along the catalytic pathway. For both OASS-A and $\beta_2$, the first half reaction occurs with the rapid formation of the external Schiff base species without detection of the *gem*-diamine species, and deprotonation of the external Schiff base $C_\alpha$ is partially rate-determining for conversion to the α-aminoacrylate. However, there is considerable divergence in the mechanism at the point of deprotonation; OASS-A appears to convert the OAS−external Schiff base directly via a concerted elimination of a proton and acetate in a process that is quasi-irreversible; whereas in the $\beta_2$ dimeric form of tryptophan synthase, the reaction of L-serine gives the external Schiff base as a rapidly formed transient which then decays to an equilibrium mixture, with a pH-dependent distribution, comprised of the external Schiff base and α-aminoacrylate (Peracchi et al., 1995; Drewe & Dunn, 1985). In the $\alpha_2\beta_2$ system, deprotonation of the L-serine external Schiff base is also partially rate-limiting, but the L-serine quinonoidal species is detected as a fleeting transient in the approach to equilibrium (Drewe & Dunn, 1985).

In the second half reaction of the OASS-A system, reaction of the α-aminoacrylate intermediate with sulfide is very rapid, and no intermediate is detected. In the $\beta_2$ system, since the L-serine external Schiff base is quasi-stable, reaction with indole is limited by deprotonation, and no intermediates are detected. However, in the $\alpha_2\beta_2$ system, the second half reaction is characterized by the rapid reaction of α-aminoacrylate with indole to give a transient quinonoidal species ($\lambda_{max}$, 476 nm) which then decays to the L-tryptophan external Schiff base ($\lambda_{max}$, 425 nm) prior to the release of L-tryptophan (Lane & Kirschner, 1983; Drewe & Dunn, 1986). The generation of quinonoidal species via reaction of the $\alpha 2\beta 2$ α-aminoacrylate with nucleophilic analogs of indole (e.g., indoline, aniline, $\beta$-mercaptoethanol, thiophenol, and hydroxylamine; Roy et al., 1988; Miles, 1979; Dunn et al., 1990; Tanaka et al., 1986; Wilcox, 1974) is a general feature of the bienzyme complex. Therefore, the absence of a quinonoidal species in the OASS-A catalytic mechanism is a surprising feature of these studies.

Some of the differences in the behavior of the OASS-A, $\beta_2$, and $\alpha_2\beta_2$ systems are likely attributable to the difference in chemical reactivity of the first substrate; the *O*-acetyl group of OAS makes this substrate chemically activated for the elimination step, whereas the hydroxyl group of L-serine is a sluggish leaving group that likely requires considerable activation to achieve elimination. Therefore, it may not be surprising that the tryptophan synthase system proceeds via the intermediacy of the L-serine quinonoid, while OASS-A carries out what appears to be a concerted elimination. The differences in ground state stabilities of the external Schiff base and α-aminoacrylate species formed respectively with OASS-A, $\beta_2$, and $\alpha_2\beta_2$ must reflect strong differences in strengths of the specific interactions, and therefore protein conformation plays a dominant role in determining the relative stabilities of the external Schiff base and α-aminoacrylate ground states. There are striking differences in the spectra of the OASS-A and $\alpha_2\beta_2$ α-aminoacrylate species; the OASS-A species exhibits a well-defined long-wavelength $\pi,\pi^*$ transition with a $\lambda_{max}$ of 470 nm (Figure 1), whereas the $\alpha_2\beta_2$ species is characterized by a $\pi,\pi^*$ transition with a $\lambda_{max}$ of 350 nm and a low-intensity shoulder extending beyond 500 nm. It is likely that the 350 nm species has a different tautomeric form compared to the OASS-A α-aminoacrylate, indicating that the sites of these two enzymes are designed to stabilize α-aminoacrylate species with different charge distributions. It is further likely that this difference in structure accounts for the difference in reactivity with nucleophiles.

## REFERENCES


Alexander, F. W., Sandmeier, E., Mehta, P. K., & Christen, P. (1994) *Eur. J. Biochem. 219*, 953−960.

Bernasconi, C. (1976) *Relaxation Kinetics*, pp 20−39, Academic Press, New York.

Cook, P. F., & Wedding R. T. (1976) *J. Biol. Chem. 251*, 2023−2029.

Cook, P. F., Hara, S., Nalabolu, S. R., & Schnackerz, K. D. (1992) *Biochemistry 31*, 2298−2303.

Drewe, W. F., Jr., & Dunn, M. F. (1985) *Biochemistry 24*, 3977−3987.

Drewe, W. F., Jr., & Dunn, M. F. (1986) *Biochemistry 25*, 2494−2501.

Dunn, M. F., Bernhard, S. A., Anderson, D., Copeland, A., Morris, R. G., & Roque, J. P. (1979) *Biochemistry 18*, 2346−2354.

Dunn, M. F., Aguilar, V., Brzovic, P. S., Drewe, W. F., Jr., Houben, D. F., Leja, C. A., & Roy, M. (1990) *Biochemistry 29*, 8598−8607.

Hara, S., Payne, M. A., Schnackerz, K. D., & Cook, P. F. (1990) *Protein Expression Purification 1*, 70−80.

Houben, K. F., & Dunn, M. F. (1990) *Biochemistry 29*, 2421−2429.

Houben, K. F., Kadima, W., Roy, M., & Dunn, M. F. (1989) *Biochemistry 28*, 4140−4147.

Koerber, S. C., MacGibbon, A. K. H., Dietrich, H., Zeppezauer, M., & Dunn, M. F. (1983) *Biochemistry 22*, 3424−3431.

Kredich, N. M., & Tomkins, G. M. (1966) *J. Biol. Chem. 241*, 4955−4965.

Kredich, N. M., Becker, M. A., & Tomkins, G. M. (1969) *J. Biol. Chem. 244*, 2428−2439.

Lane, A. N., & Kirschner, K. (1983) *Eur. J. Biochem. 129*, 561−570.
McClure, G. D., Jr., & Cook, P. F. (1994) *Biochemistry 33*, 1674−1683.
Metzler, C. M., Cahill, A. E., Petty, S., Metzler, D. E., & Lang., L. (1985) *Appl. Spectrosc. 39*, 333−339.
Metzler, C. M., Viswanath, R., & Metzler, D. E. (1991) *J. Biol. Chem. 266*, 9374−9381.
Miles, E. W. (1979) *Adv. Enzymol. Relat. Areas Mol. Biol. 49*, 127−186.
Peracchi, A., Bettati, S., Mozzarelli, A., Rossi, G. L., Miles, E. W., & Dunn, M. F. (1995) *Biochemistry* (submitted for publication).
Roy, M., Keblawi, S., & Dunn, M. F. (1988) *Biochemistry 27*, 6698−6704.
Schnackerz, K. D., Ehrlich, J. H., Giessman, W., & Reed, T. A. (1979) *Biochemistry 18*, 3557−3563.
Schnackerz, K. D., Tai, C.-H., Simmons, J. W., III, Jacobson, T. M., Rao, G. S. J., & Cook, P. F. (1995) *Biochemistry 34*, 12152−12160.
Siano, D. B. (1972) *J. Chem. Educ. 49*, 755−757.
Siano, D. B., & Metzler, C. M. (1969) *J. Chem. Phys. 51*, 1851−1861.
Tai, C.-H., Nalabolu, S. R., Jacobson, T. M., Minter, D. E., & Cook, P. F. (1993) *Biochemistry 32*, 6433−6442.
Tai, C.-H., Nalabolu, S. R., Simmons, J. W., III, Jacobson, T. M., & Cook, P. F. (1995) *Biochemistry 34*, 12311−12322.
Tanaka, H., Tanizawa, K., Takahiro, A., Saito, K., Arai, T., & Soda, K. (1986) *FEBS Lett. 196*, 357−360.
Woehl, E. U., & Dunn, M. F. (1995) *Biochemistry 34*, 9466−9476.
Wilcox, M. (1974) *Anal. Biochem. 59*, 436−440.

BI952938O